Acta Radiologica Open
7(10) 1–5

DOI: 10.1177/2058460118806657
journals.sagepub.com/home/arr
SAGE

Testicular seminoma in the aged rat visualized by phase-contrast X-ray computed tomography

Thet-Thet-Lwin[1,2], Akio Yoneyama[3], Motoki Imai[2], Hiroko Maruyama[1,2], Kazuyuki Hyodo[4] and Tohoru Takeda[1,2]

Abstract

Spontaneously growing testicular seminoma in the aged rat was imaged by one of the most sensitive imaging modalities, namely, phase-contrast X-ray computed tomography (CT) with crystal X-ray interferometry. Phase-contrast X-ray CT clearly depicted the detailed inner structures of the tumor and provided 20× magnified images compared to light-microscopic images. Phase-contrast X-ray CT images are generated based on density variations in the object, whereas pathological images are based on differentiation of cellular structures, such as the cellular nuclei and cytoplasm. The mechanism of image generation differs between the two techniques: phase-contrast X-ray CT detects even minute differences in the density among pathological structures, depending, for example, on the number and sizes of the nuclei, variations of the cytoplasmic components, and presence/absence of fibrous septa, cystic changes, and hemorrhage. Thus, phase-contrast X-ray CT with a spatial resolution of 26 μm might allow prediction of the morphological characteristics of a tumor even before histopathological processing.

Keywords

Seminoma, aged rat, crystal X-ray interferometry-based phase-contrast X-ray CT

Received 9 July 2018; accepted 22 September 2018

Introduction

The incidence of testicular cancer, the most frequently encountered cancer among younger men, has been increasing steadily over the last 40 years (1). In cancer research, tumor models are mostly generated by implanting the tumor cells into the target organ, because of the rare natural occurrence of these tumors. At our laboratory, while we were engaged in research on the effects of aging, we accidentally detected masses in the testicles of either side of an otherwise healthy two-year-old Wistar rat. In a previous two-year carcinogenicity study involving 1261 male Wistar rats, the incidence of testicular tumors during the study period was reported to be approximately 7.2% (2).

Preclinical tumor imaging in an animal model plays an important role in the evaluation of the growth, progression, metastatic pattern, and therapy of the tumor. In the currently used conventional absorption X-ray imaging technique, image contrast is generated based on attenuation differences among the tissues within an object. Tumors are mostly composed of soft tissues, which show significantly low attenuation, and it is very difficult to distinguish the detailed inner structure of the tumor, even using a contrast agent. Thus, a high contrast resolution imaging technique is indispensable to observe the detailed morphological characteristics of tissues. The phase-contrast X-ray imaging technique enables visualization of soft tissues with high contrast and spatial resolution. In phase-contrast X-ray imaging

[1]School of Allied Health Sciences, Kitasato University, Kanagawaken, Japan
[2]Graduate School of Medical Sciences, Kitasato University, Kanagawaken, Japan
[3]SAGA Light Source, Kyushu Synchrotron Light Research Center, Saga, Japan
[4]Institute of Materials Structure Science, High Energy Accelerator Organization (KEK), Ibarakiken, Japan

Corresponding author:
Thet-Thet-Lwin, School of Allied Health Sciences, Graduate School of Medical Sciences, Kitasato University, 1-15-1 Kitasato, Minamiku, Sagamiharashi, Kanagawaken 252-0373, Japan.
Email: ttlwin@kitasato-u.ac.jp

based on the phase shift of the X-ray, the density resolutions for elements with low atomic numbers, such as H, C, N and O, are approximately 1000 times higher than those in absorption X-ray imaging (3). Although, many phase-contrast X-ray imaging techniques (4–7) have been used for biomedical imaging studies, crystal X-ray interferometry-based phase-contrast X-ray computed tomography (CT) provides the highest sensitivity resolution as compared to other methods and enables fine observation of soft tissues (8–12).

Here, very rare spontaneous growing testicular masses in an aged rat were examined by crystal X-ray interferometry-based phase-contrast X-ray CT imaging, to investigate whether this imaging modality would allow differentiation of the morphological structures in the testicular tumor as clearly as histopathological images.

Case report

Animal

Asymmetrically enlarged testicles were incidentally observed in an otherwise healthy two-year-old Wistar rat during the course of one of our studies. No abnormal lesions were observed in any other organs, including the brain, lung, heart, liver, kidney, or spleen. For phase-contrast X-ray CT imaging, the testes were extracted from the animals after transcardiac perfusion of physiological saline with heparin and fixed using 10% formalin.

Phase-contrast X-ray imaging

The experiment was performed at the vertical wiggler beamline of the Photon Factory, Tsukuba, Japan. A two-crystal X-ray interferometry-based phase-contrast X-ray imaging system was used. The X-ray charge-coupled device camera with a 1300×1000-pixel sensor had a pixel size of $13 \times 13\,\mu m^2$. The field of view was $16 \times 13\,mm^2$. During the phase-contrast imaging, the excised testicles were placed in a sample cell filled with formalin to prevent drying of the samples. The X-ray energy was set at 35 keV. The exposure time was 5 s for each interference pattern and 250 projections were delivered over 180°. The density and spatial resolution of the phase-contrast X-ray CT system that we used were approximately $0.5\,mg/cm^3$ and 26 μm, respectively (9).

Numerical evaluation of the three-dimensional (3D) image data was conducted using a volume-rendering software (Real INTAGE; KGT Inc., Tokyo, Japan). A gray value of 30% was chosen as the cutoff for viewing the intra-tumoral vessels.

Histopathological staining

After the phase-contrast X-ray imaging, testicular masses were cut 3-μm thick and hematoxylin and eosin (H&E) staining, reticulum staining, and placental alkaline phosphatase (PLAP) immunostaining were carried out. The stained sections were imaged using an optical microscope (Olympus FSX100; Olympus, Tokyo, Japan).

The original H&E color images were converted into 8-bit gray-scale images. The nuclei became dark, whereas the cytoplasm and extracellular matrix showed varying shades of gray. These pathological gray-scale images were compared with the phase-contrast X-ray CT images.

Phase-contrast X-ray CT image and histopathological findings

Phase-contrast X-ray CT images of the testes revealed heterogeneity of multiple lesions embedded in the seminiferous tubules, found to be closely similar to the gray-scale H&E-stained histopathological images (hereinafter, simply referred to as H&E images).

Phase-contrast X-ray CT images of the testis containing the tumor revealed three masses of different sizes and densities embedded in the seminiferous tubules (Fig. 1a). The largest mass was mostly vascularized and observed as a high-density lesion, with a few low-density areas. The intermediate-sized mass was visualized as a moderately low-density lesion, with cyst-like low densities encapsulated by high-density septa in some parts of the periphery. The smallest mass was visualized as a low-density lobulated lesion with a central high-density area. Surrounding seminiferous tubules of various sizes and shapes were seen. The H&E images showed three different tumor masses with various degrees of cellularity. The largest mass showed heterogeneous cellularity and a lobulated area with dense septa. The intermediate-sized mass showed relatively homogeneous cellularity with densely capsulated lobules in a part of the periphery. The smallest mass was lobulated and was composed of clear cells, with central lymphocytic infiltration (Fig. 1b and c). In addition, the intra-tumoral vessel network within the rounded lesion surrounded by a blue square (Fig. 1a) was clearly depicted by 3D reconstruction (Fig. 1d and e).

In the phase-contrast X-ray CT, absolute densities can be calculated (9) for understanding the mean density variations within the tumors. Regions of interest 1, 2, and 3 within the tumor (Fig. 1a) had different densities as $1.062 \pm 0.001\,g/cm^3$, $1.066 \pm 0.001\,g/cm^3$, and $1.040 \pm 0.006\,g/cm^3$, receptively. These different

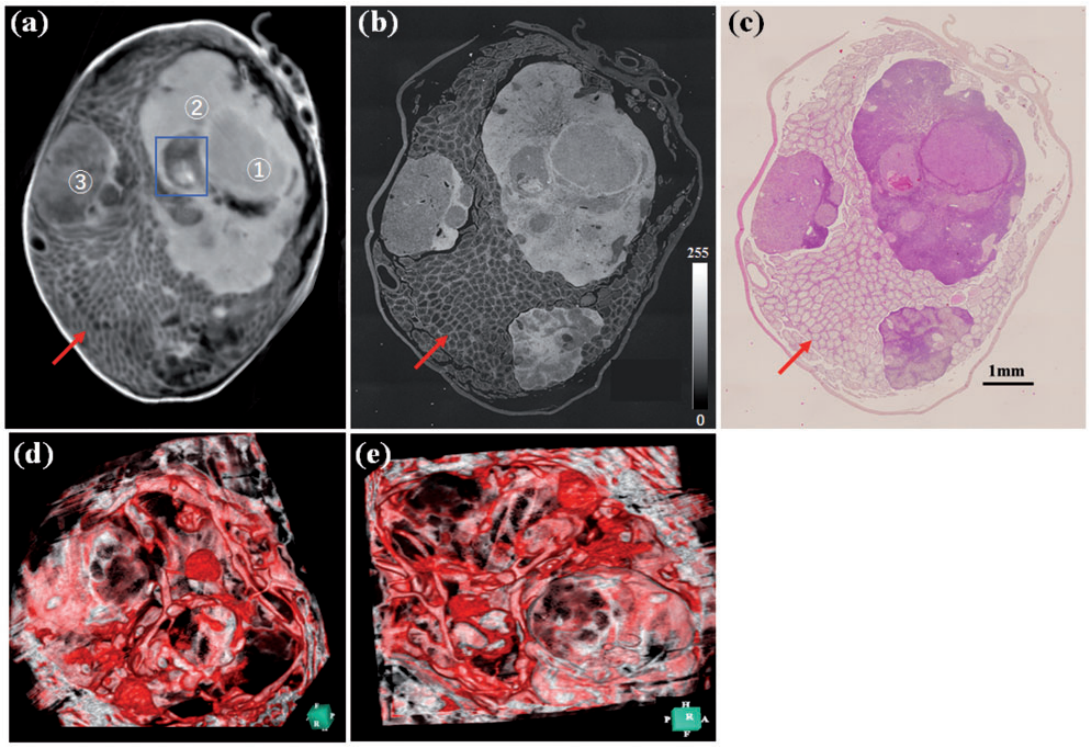

Fig. 1. Testis with the smaller tumors: (a) phase-contrast X-ray CT image; (b) corresponding histological (H&E) gray-scale image; (c) color image. Masses of three different sizes of heterogeneous densities embedded in seminiferous tubules (red arrow). Areas of interest in the phase-contrast X-ray CT image (a): 1) tumor area 1; 2) tumor area 2; 3) tumor area 3. Three-dimensional reconstruction of the region within the blue square in the phase-contrast X-ray CT image (a) to view the vascular network of the tumor in a different direction (d, e).

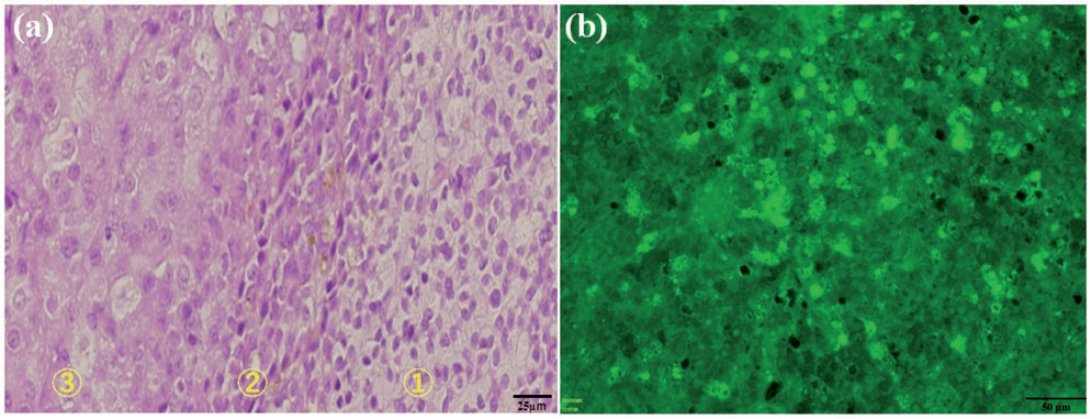

Fig. 2. Histopathological sections of the tumor: (a) H&E stained image showing different types of neoplastic cells; (b) immunostained image showing positive staining of the tumor cells for placental alkaline phosphatase, a tumor marker for human seminoma.

densities were corresponded to the various types of neoplastic cells seen on the H&E images.

Different types of neoplastic cells were observed, including: (i) cells with large clear cytoplasm and small hyperchromatic nuclei; (ii) densely infiltrating lymphocytes with hyperchromatic nuclei and a small volume of relatively enhancing cytoplasm; and (iii) large, round to polyhedral cells with moderately enhancing large cytoplasm and relatively large hypochromatic nuclei (Fig. 2a). The final pathological diagnosis was determined to be seminoma based on the results of fluorescent immunostaining for placental alkaline phosphatase (13) (Fig. 2b). Reticulum staining yielded a negative result (data are not shown), based on

which the diagnosis of testicular lymphoma was excluded.

Discussion

The testicular tumors in the present study were diagnosed by histopathological examination as germ cell tumors, possibly seminoma (14,15). Interstitial cell tumors are usually known to occur in the rat testis, and germ cell tumors, such as seminoma, are exceedingly rare (16). According to one report, the incidence of seminoma in 31,868 rats of several strains was 0.003% (17).

Phase-contrast X-ray CT clearly depicted the spontaneously growing seminoma in the aged rat without the need for use of any contrast agent, and the images closely resembled 20× magnified gray-scale H&E images. However, the phase-contrast X-ray CT images appeared slightly degraded as compared to the gray-scale H&E images, probably due to the relatively large slice thickness: 26 μm in the phase-contrast images versus 3 μm in the histopathological images. Phase-contrast X-ray CT allowed visualization of various components of the tumors, such as the solid tumor components, cysts, and septa, based on density variations. Phase-contrast X-ray CT images are generated by density differences within the object, whereas gray-scale H&E images show cellular morphological components, such as nuclei of various chromaticities, and cytoplasm sizes. The density differences within the solid components might be mainly generated by the number and sizes of the nuclei per unit area and the amounts of protein within the cytoplasm. Thus, minute differences in the absolute densities within the tumor might predict the characteristics of a tumor and its malignancy grade.

Pathological images provide abundant information about micro-structures; however, deformities or artifacts are occasionally caused during the cutting and staining procedures. Furthermore, phase-contrast X-ray CT allowed discrimination of minute differences of the absolute densities within the tumor and also a 3D volumetric study.

White spots within the tumors visualized on phase-contrast X-ray CT images corresponded to blood clots within vessels visualized on the H&E images. Transaxial phase-contrast X-ray CT images failed to reveal the vascular network within the tumor, which is a unique vital component of the tumor (18); therefore, 3D image reconstruction was performed. This 3D information about the tumor vessels is useful, because the density of the vascular network is known to be related to the histological malignancy grades of seminomas (19).

In conclusion, phase-contrast X-ray CT allowed clear visualization of the detailed inner structures and the 3D vascular network in the seminomas, a rarely encountered germ cell tumor, in the rat. These images are equivalent to low magnified histopathological images. Thus, phase-contrast X-ray CT with a spatial resolution of 26 μm might allow prediction of the morphological characteristics of a tumor even before histopathological processing.

Acknowledgements

The authors thank Associate Professor Khin Moe Kywe, Defence Services Medical Academy, Myanmar for advice to pathological diagnosis. This research was carried out under the approval (proposal nos. 2016G034, 2017G171) of the committee of the High Energy Accelerator Research Organization and the experimental protocol was approved by the President of Kitasato University through the judgment of the Animal Care and Use Committee of Kitasato University (approval no. 104-02).

Declaration of conflicting interests

The authors declared no potential conflicts of interest with respect to the research, authorship, and/or publication of this article.

Funding

The author(s) received no financial support for the research, authorship, and/or publication of this article.

ORCID iD

Thet-Thet-Lwin http://orcid.org/0000-0002-7225-9228

References

1. Huyghe E, Matsuda T, Thonneau P. Increasing incidence of testicular cancer worldwide: a review. *J Urol* 2003;170:5–11.
2. Bomhard E, Rinke M. Frequency of spontaneous tumours in Wistar rats in 2-year studies. *Exp Toxicol Pathol* 1994;46:17–29.
3. Takeda T, Momose A, Itai Y, et al. Phase-contrast imaging with synchrotron X-rays for detecting cancer lesions. *Acad Radiol* 1995;2:799–803.
4. Momose A. Demonstration of phase-contrast X-ray computed tomography using an X-ray interferometer. *Nuclear Instruments and Methods in Physics Research Section A: Accelerators, Spectrometers, Detectors and Associated Equipment* 1995;352,622–628.
5. Momose A, Kawamoto S, Koyama I, et al. Demonstration of x-ray Talbot interferometry. *Jpn J Appl Phys* 2003;42:L866–868.
6. Koyama I, Momose A, Wu J, et al. Biological imaging by X-ray phase tomography using diffraction-enhanced imaging. *Jpn J Appl Phys* 2005;44:8219–8221.
7. Cloetens P, Ludwig W, Baruchel J. Holotomography: Quantitative phase tomography with micrometer resolution using hard synchrotron radiation x rays. *Appl Phys Lett* 1999;75:2912–2914.
8. Yoneyama A, Baba R, Hyodo K, et al. Quantitative comparison of performance of absorption, Talbot

interferometric, and crystal x-ray interferometric imaging. Electronic Presentation Online System. In: Proceedings of the ECR 2015 Conference of the European Society of Radiology; 4–8 March 2015, Vienna. Austria. Available at: http://dx.doi.org/10.1594/ecr2015/C-0531.
9. Yoneyama A, Wu J, Hyodo K, et al. Quantitative comparison of imaging performance x-ray interferometric imaging and diffraction enhanced imaging. *Med Phys* 2008;35:4724–4734.
10. Momose A, Takeda T, Itai Y, et al. Phase-contrast x-ray computed tomography for observing biological soft tissues. *Nat Med* 1996;2:473–475.
11. Takeda T. Momose A, Hirano K, et al. Human carcinoma: early experience with phase-contrast x-ray CT with synchrotron radiation: comparative specimen study with optical microscopy. *Radiology* 2000;214:298–301.
12. Lwin TT, Yoneyama A, Hara A, et al. Spontaneous brain tumor imaging of aged rat by crystal X-ray interferometer-based phase-contrast X-ray CT. *Acta Radiol Open* 2016;5:2058460115626958.
13. Emerson RE, Ulbright TM. Intratubular germ cell neoplasia of the testis and its associated cancers: the use of novel biomarkers. *Pathology* 2010;42:344–355.
14. Creasy D, Bube A, de Rijk E, et al. Proliferative and nonproliferative lesions of the rat and mouse male reproductive system. *Toxicol Pathol* 2012;40:40S–121S.
15. Boorman GA, Rehm S, Waalkes MP, et al. Seminoma, testis, rat. In: TC U Jones, RD Hunt, eds. *Monographs on Pathology of Laboratory Animals, Genital System*. Berlin: Springer, 1987:192–195.
16. Kerlin RL, Roesler AR, Jakowski AB, et al. A poorly differentiated germ cell tumor (seminoma) in a long Evans rat. *Toxicol Pathol* 1998;26:691–694.
17. Curtis MR, Bullock FD, Dunning WF. A statistical study of the occurrence of spontaneous tumors in a large colony of rats. *Am J Cancer* 1931;15:67–121.
18. Zetter BR. Angiogenesis and tumor metastasis. *Annu Rev Med* 1998;49:407–424.
19. Restucci B, Maiolino P, Paciello O, et al. Evaluation of angiogenesis in canine seminomas by quantitative immunohistochemistry. *J Comp Pathol* 2003;128:252–259.